Gadolinium nanoparticles and contrast agent as radiation sensitizers

2015 Phys. Med. Biol. 60 4449

(http://iopscience.iop.org/0031-9155/60/11/4449)

IOP Publishing | Institute of Physics and Engineering in Medicine Physics in Medicine & Biology

Phys. Med. Biol. **60** (2015) 4449–4464 doi:10.1088/0031-9155/60/11/4449

Gadolinium nanoparticles and contrast agent as radiation sensitizers

Florence Taupin[1,2,3,4,5,13], Mélanie Flaender[1,2,5,13], Rachel Delorme[6,7], Thierry Brochard[5], Jean-François Mayol[8], Josiane Arnaud[9], Pascal Perriat[10], Lucie Sancey[11], François Lux[11], Rolf F Barth[12], Marie Carrière[3,4], Jean-Luc Ravanat[3,4] and Hélène Elleaume[1,2,5]

[1] Université Grenoble Alpes, Grenoble Institut des Neurosciences, GIN, F-38000 Grenoble, France
[2] Inserm, U836, F-38000 Grenoble, France
[3] Université Grenoble Alpes, INAC-SCIB, LAN, F-38000 Grenoble, France
[4] CEA, INAC-SCIB, F-38000 Grenoble, France
[5] European Synchrotron Radiation Facility, F-38000 Grenoble, France
[6] LIST, Laboratoire d'Intégration de Systèmes et des Technologies, CEA Saclay, France
[7] Université Grenoble-Alpes, LPSC, CNRS/IN2P3, F-38000 Grenoble, France
[8] Institut de Recherche Biomédicale des Armées, F-38700 La Tronche, France
[9] CHU de Grenoble, F-38000 Grenoble, France
[10] Laboratoire Matériaux Ingénierie et Sciences, Université de Lyon, INSA, UMR 5510, F-69000 Lyon, France
[11] Institut Lumière Matière, UMR5306 Université Lyon 1-CNRS, Université de Lyon, F-69622 Villeurbanne Cedex, France
[12] Department of Pathology, The Ohio State University, Columbus, OH 43210, USA

E-mail: h.elleaume@esrf.fr

Received 21 January 2015, revised 31 March 2015
Accepted for publication 16 April 2015
Published 19 May 2015

Abstract

The goal of the present study was to evaluate and compare the radiosensitizing properties of gadolinium nanoparticles (NPs) with the gadolinium contrast agent (GdCA) Magnevist® in order to better understand the mechanisms by which they act as radiation sensitizers. This was determined following either low energy synchrotron irradiation or high energy gamma irradiation of F98 rat glioma cells exposed to ultrasmall gadolinium NPs (GdNPs, hydrodynamic diameter of 3 nm) or GdCA. Clonogenic assays were used to quantify cell survival after irradiation in the presence of Gd using monochromatic x-rays with energies in the 25 keV–80 keV range from a synchrotron and 1.25

[13] Both authors equally contributed to the manuscript.

MeV gamma photons from a cobalt-60 source. Radiosensitization was demonstrated with both agents in combination with X-irradiation. At the same concentration (2.1 mg mL^{-1}), GdNPS had a greater effect than GdCA. The maximum sensitization-enhancement ratio at 4 Gy (SER_{4Gy}) was observed at an energy of 65 keV for both the nanoparticles and the contrast agent (2.44 ± 0.33 and 1.50 ± 0.20, for GdNPs and GdCA, respectively). At a higher energy (1.25 MeV), radiosensitization only was observed with GdNPs (1.66 ± 0.17 and 1.01 ± 0.11, for GdNPs and GdCA, respectively). The radiation dose enhancements were highly 'energy dependent' for both agents. Secondary-electron-emission generated after photoelectric events appeared to be the primary mechanism by which Gd contrast agents functioned as radiosensitizers. On the other hand, other biological mechanisms, such as alterations in the cell cycle may explain the enhanced radiosensitizing properties of GdNPs.

Keywords: gadolinium, nanoparticles, contrast agent, photoelectric effect, radiosensitization, x-rays

(Some figures may appear in colour only in the online journal)

Background

High grade gliomas are the most common primary malignant brain tumor in adults. They are almost invariably fatal with the current standard therapy consisting of surgery, radiotherapy and the concomitant administration of temozolomide (TMZ) followed by repetitive cycles of the latter (Stupp *et al* 2005, 2009). Although the increase in overall median survival was only 2.5 months (14.6 versus 12.1 months), approximately 25% of patients were still alive at 2 years compared to less than 10% for those who did not received TMZ. The poor prognosis of patients with high grade gliomas highlights the necessity of evaluating new therapeutic approaches. Nanoparticles (NPs) are being evaluated as theranostics for radiation therapy. Hainfeld *et al* (2010) have shown that gold nanoparticles (AuNPs) could enhance the efficacy of radiation therapy for the treatment of the EMT-6 murine mammary carcinoma, and more recently, a murine brain tumor (Hainfeld *et al* 2013). This therapeutic approach, initially proposed by Norman *et al* (1991) was based on the principle that the physical dose delivered locally to a tumor could be enhanced by the photon interactions that would occur within a tumor that had been loaded with high-*Z* atoms (Boudou *et al* 2005, Mesa *et al* 1999). The first studies were performed using molecular contrast agents and low energy x-rays (<100 keV), where the photoelectric effect's cross-section was maximal compared to water. In the present study we have used gadolinium (Gd) either in a molecular or nanoparticle form. Gd has been used widely as a clinical contrast agent, and also as a photoactivator (De Stasio *et al* 2001, Pignol *et al* 2003). When irradiated with x-rays, high *Z* elements generate electrons that have a kinetic energy equal to the difference between the incident photons' energy and the electron binding energies. For example, K-edge photoelectrons (20 keV), created by photoionization of Gd atoms (Gd K-edge: 50.24 keV) by 70 keV photons, have a mean pathlength in water of ~8 μm, which is similar to the diameter of a cell. Electron range in water versus energy can be found in NIST/ESTAR www.nist.gov/pml/data/star/. Extracellular high-*Z* atoms could have a direct effect on cell survival if a sufficient number of these atoms was localized in proximity to or within the cell. Following a K-edge photoelectric event, K-shell vacancies are created and subsequently filled with higher orbital electrons. The electronic re-organization of the atoms

yields a cascade of either fluorescence x-rays or Auger electrons that have very low energies, which are deposited very close to their site of production (Karnas *et al* 2001, Terrissol *et al* 2004). If the high-*Z* atoms remain external to the cell nucleus, the probability that Auger electrons interact with the nucleus is low, however, they could damage other cellular targets such as the cell membrane and mitochondria.

Using higher energies, such as those produced by a linear accelerator (LINAC), the photoelectric effect would no longer predominate and much lower dose enhancement factors (DEFs) would be expected. Monte Carlo simulations have been developed to evaluate the physical dose-enhancement induced by the presence of the high *Z* elements, based on their distribution (Solberg *et al* 1992, Mesa *et al* 1999, Robar *et al* 2002, Ceberg *et al* 2012). For example, Robar *et al* (2002) have reported on the DEFs simulated in a numeric head phantom for different Gd concentrations in the tumor as a function of the radiation energy. The calculated DEFs were 1.2 and 5.3 for a 2 MeV or 60 keV x-ray beam, respectively, with 30 mg of Gd per gram of tumor (Robar *et al* 2002). The calculated and experimental DEFs were found to be in good agreement at a macroscopic scale in other studies (Corde *et al* 2005, Gastaldo *et al* 2008).

Although most studies refer to larger DEFs in the keV range, as predicted theoretically, radiosensitization at MeV photon energies also has been reported with NPs (McMahon *et al* 2008, Tsiamas *et al* 2013). Jain *et al* (Jain *et al* 2011, Coulter *et al* 2012) have observed dose enhancement greater than MC simulations after irradiation of MDA-MB-231 breast cancer cells at MeV photon energies with 1.9 nm AuNPs. However, contradictory results also have been reported depending on the energy range considered (Butterworth *et al* 2010, 2012, McMahon *et al* 2011b, 2012, Lechtman *et al* 2013). Recently, ultrasmall GdNPs have been utilized as radiosensitizers for various tumor cells (Mowat *et al* 2011, Stefancikova *et al* 2014, Luchette *et al* 2014, Miladi *et al* 2015). The NPs consisted of a core of gadolinium oxide surrounded by a shell of polysiloxane and were functionalized by either DTPA or 1,4,7,10-tetraazacyclododecane-1,4,7,10-tetraacetic acid (DOTA). These nanoparticles also have been used *in vivo* for the treatment of 9 L gliosarcoma bearing rats in combination with x-ray microbeams ($E < 150$ keV) (Le Duc *et al* 2011). The median survival time was extended to 90 d compared to 47 d for irradiation alone. The underlying mechanisms by which radiosensitization increased in presence of the NPs following irradiation are still unclear. Monte Carlo simulations have shown that the assembly of heavy atoms within the NPs strongly modified the dose patterns at the nanoscale level (Lechtman *et al* 2013, McMahon *et al* 2011a, 2011b, 2012, Lin *et al* 2014). Radiation doses were found to be higher within a few nanometers surrounding the NPs compared to those measured in water when using either high energy (MeV) x-rays or those in the photoelectric domain. Importantly, simulations at the nanoscale predicted that the enhancement was few order of magnitudes greater using kilovoltage energies compared to high energy x-rays (Roeske *et al* 2007, McMahon *et al* 2011b, Butterworth *et al* 2012, Lechtman *et al* 2013). Since the physical DEF is strongly energy dependent, both at the macroscopic or nanoscopic scale (Karnas *et al* 1999, Karnas *et al* 2001, Boudou *et al* 2005, 2007, Robar *et al* 2006, Gastaldo *et al* 2008, Lechtman *et al* 2013, Mesbahi *et al* 2013), monochromatic radiation produced by a synchrotron source provides a unique tool for evaluating the mechanisms by which radiosensitization occurs. Furthermore, this can be used to differentiate between physical and biological contributors to radiosensitization.

The aim of the present study was to evaluate, *in vitro,* the radiosensitizating effects produced by ultrasmall GdNPs compared to those produced by the gadolinium contrast agent Magnevist®. Clonogenic assays were performed using different incubation and irradiation

conditions with either monochromatic x-rays from a synchrotron source (7 energies from 25 keV to 85 keV) or a cobalt-60 source (1.25 MeV).

Our final goal was to optimize the choice of a radiosensitizers for obtaining the maximal dose-enhancement in radiotherapy for the treatment of brain tumors. From previous studies, it is known that Magnevist® is rapidly eliminated from the tissue (Gd $T_{1/2}$ ~ 30 min in brain tumors) (Le Duc *et al* 2004, Cao *et al* 2006). On the other hand, we have observed much longer retention times with GdNPs in preliminary studies performed using F98 glioma implanted into the brains of syngeneic Fischer rats and the GdNPs used in the present study. We have observed that Gd is eliminated from the brain tumor following an exponential decay ($C = C_0 \exp(-t/\zeta)$) with a time constant of ζ ~300 min. Therefore, to match the conditions that could be obtained *in vivo*, we chose different incubation conditions for GdNPs and GdCA. Magnevist® was present in the culture medium only during the irradiation time i.e. ~20 min and cells were incubated for 5 h with GdNPs before irradiation.

Methods

Gadolinium compounds

GdNPs were provided by the laboratory of O. Tillement (Institut Lumière Matière, univ Lyon, 69622 Villeurbanne cedex, France). These nanoparticles are made of a polysiloxane matrix and surrounded by gadolinium chelates (diethylenetriaminepentaacetic acid (DTPA)) covalently grafted to the polysiloxane inorganic matrix. A detailed description of their synthesis and properties has been reported elsewhere (Di Corato *et al* 2013). To briefly summarize, a gadolinium oxide core was obtained in a first step by addition of soda on gadolinium trichloride in diethylene glycol at room temperature. The growth of a polysiloxane shell was ensured by sol gel process. The nanoparticles displayed a sub-5 nm hydrodynamic diameter of approximatively 3.0 ± 1.0 nm.

The Gd contrast agent (GdCA) Magnevist® a complex of Gd with a chelating agent, DTPA, was purchased from Bayer Schering Pharma, Berlin, Germany. Its chemical formula is $C_{28}H_{54}GdN_5O_{20}$ with molecular weight of 938 Da.

F98 cells

F98 glioma cells were purchased from the American Type Culture Collection, Manassas, VA (ATCC, # CRL-2397) and they have been described in detail by Barth and Kaur (Barth and Kaur 2009). These cells have a highly invasive pattern of growth within the brains and are weakly immunogenic in syngeneic Fischer rats (36).

Determination of gadolinium nanoparticles uptake

Gd uptake was determined by means of inductively coupled plasma-mass spectrometry (ICP-MS) using a Thermo X serie II, spectrometer (Thermo Electron, Bremen, Germany), which was equipped with an impact bead spray chamber and a standard nebulizer (1 mL min^{-1}). Three different treatment times were investigated, 30 min, 2 h and 5 h, following incubation with GdNPs at a concentration of 2.1 mg Gd mL^{-1}. For Gd determinations, the cells were washed twice in PBS, trypsinized (Trypsine EDTA 0.05%—Invitrogen), suspended in 1 mL of PBS, and then counted. Nitric acid was then added to the cell suspensions (final concentration 1%) and Gd concentrations were determined using an external calibration curve. Two stable

Gd isotopes (^{155}Gd and ^{157}Gd) were measured and rhodium (^{103}Rh) was used as an internal standard. Determinations were carried out in triplicate.

Cell cycle distribution

The effects of incubation with GdNPs (2.1 mg mL^{-1}, 5 h) on the cell cycle of F98 glioma cells was determined from DNA histograms obtained by flow cytometric analysis. After incubation, the culture medium was decanted and the cells were trypsinized, washed twice with PBS and fixed with a 2% formalin solution. Cell membranes were permeabilized with 0.2% Triton X-100 in PBS. DNA was determined by fluorescent staining with DAPI (10 μg mL^{-1}) with a flow cytometer (LSR II, BD Bioscience, Franklin Lakes, USA). Cell cycle distribution was determined either immediately after incubation with GdNPs or after additional 24 h in a GdNPs free culture medium and compared to untreated control cells. Cell cycle analysis was performed after doublet exclusion using FlowJo software (Tree Star, INC. Ashland, OR) and Watson DNA peak deconvolution.

Cell irradiations

Three treatment conditions were evaluated: (1) untreated control cells; (2) cells incubated for 5 h with 2.1 mg mL^{-1} GdNPs and irradiated; and (3) cells irradiated in the presence of 2.1 mg mL^{-1} GdCA (Magnevist®). For GdNPs experiments, before irradiation the cells were trypsinized, washed and re-suspended in 200 μL of DMEM complete media containing the GdNPs and irradiated in Eppendorf tubes. Low energy monoenergetic x-rays (from 25 to 80 keV) were produced from a synchrotron source at the European Synchrotron Radiation Facilty (ESRF—biomedical ID17 beamline—$\Delta E/E \approx 0.1\%$). The dosimetry was performed using an ionization chamber (PTW Semiflex ion chamber 31010 − 0.125 cm^3). High energy irradiations were carried out using a cobalt-60 source, which emitted gamma photons with energies of 1.17 and 1.33 MeV (1.25 MeV mean energy). For radiosensitization versus photon energy, cells were irradiated at a single 4 Gy dose with beam energy 31.0, 40.0, 49.5, 51.0, 65.0, 80.0 keV and 1. 25 MeV. For dose-response curves, samples were irradiated with 0, 2, 4 or 6 Gy and with a beam energy of 51 keV (just above the Gd K-edge).

Clonogenic assays

Clonogenic assays were used for determining the sensitizing enhancement produced by Gd in combination with X-irradiation. Following treatment, the cells were counted and diluted in the appropriate volume of DMEM. Three different cells concentrations were seeded in triplicate into Petri dishes (100 mm diameter) containing 8 mL of complete DMEM, and they were incubated at 37 °C in an atmosphere containing 95% air and 5% CO_2 for 11 d. All experiments were repeated three times. Following staining with crystal violet, colonies of greater than 50 cells were enumerated. The surviving fractions (SF) were determined as the ratio of the number of colonies counted divided by the number of cells plated, normalized to unirradiated controls.

Cell survival and sensitization-enhancement ratio

Radiation dose response curves obtained at 51 keV were fitted by the linear quadratic (LQ) model:

$$\mathrm{SF} = \mathrm{e}^{-(\alpha D + \beta D^2)} \quad (1)$$

with, D (Gy) the radiation dose, SF the normalized survival fraction and two parameters, α (Gy^{-1}) and β (Gy^{-2}). The α parameter characterizes the first part of the slope of the cell survival curve and the effectiveness at low doses, while β represents the contribution from cumulative damages, presumably due to the interaction of two or more lesions. The α/β ratio represents the dose at which the linear and quadratic terms contribute equally to the total effect. The SER was calculated as the ratio of the Survival fraction for control cells (computed with the corresponding α and β parameters) to that of cells irradiated in combination with Gd. The SER_{4Gy} was defined as the ratio of the SF for control cells (4 Gy irradiation alone) to that of cells irradiated with 4 Gy with Gd.

Statistical analysis

All experiments were performed 3 times with triplicate samples in each study and the final data represented the means from the three independent experiments. The statistical errors on the SER_{4Gy} were evaluated taking into account the error propagation, with the formula:

$$\sigma_{SER} = \left| \frac{S_{Control}}{S_{Gd}} \right| \times \sqrt{\left(\frac{\sigma_{S_{Control}}}{S_{Control}} \right)^2 + \left(\frac{\sigma_{S_{Gd}}}{S_{Gd}} \right)^2} \quad (2)$$

Statistical differences between the experimental results were evaluated using Student's two-tailed t-test. Differences were considered significant at the level of $p \leq 0.05$.

Computed macroscopic dose-enhancement factor (DEF)

Monte Carlo simulations (PENELOPE, 2011 version) were used to estimate the macroscopic physical dose enhancement produced by Gd during irradiation. PENELOPE is a general-purpose Monte Carlo code for the coupled simulation of electron, positron and photon transport. It allows transportation of charged particles in the energy range of 50 eV–1 GeV and is based on a mixed procedure that combines detailed simulation of hard events with the continuous slowing-down approximation for soft interactions. The input geometry is defined by a cube (1 cm^3) containing either water or a solution of Gd mixed homogeneously in water at a concentration of 2.1 mg Gd mL^{-1}. The DEF was defined as the ratio between the doses deposited in the cube containing Gd to that deposited in a cube only containing water. DEFs were calculated for thirty energies covering those used for cell irradiations, between 10 keV to 2 MeV and using 10^8 incident photons per irradiation to obtain uncertainties <1%. The photon source was a square monochromatic source (1 × 1 cm) centered on the cube and placed at a distance of 1 cm in front of it. Because we only were interested on the mean macroscopic dose enhancement produced by the Gd, we choose here a low-energy electron cut-off of 1 keV for time saving reasons. The use of other MC codes such as Geant4-DNA (Incerti *et al* 2010) or dedicated MC track-structure codes like PARTRAC (Dingfelder *et al* 2008) and KURBUC (Liamsuwan *et al* 2012) that follow electrons down to the excitation threshold of water ~7–8 eV, would be necessary if the goal was to evaluate the nano-scale pattern of energy deposition.

Computed sensitization-enhancement ratio

The theoretical SER was calculated, assuming that radio-sensitization in presence of Gd was uniquely induced by physical effects. The normalized survival fraction in presence of Gd (SF_{Gd}) was calculated using the parameters α and β (obtained from the $SF_{control}$) and the computed DEF, as follows:

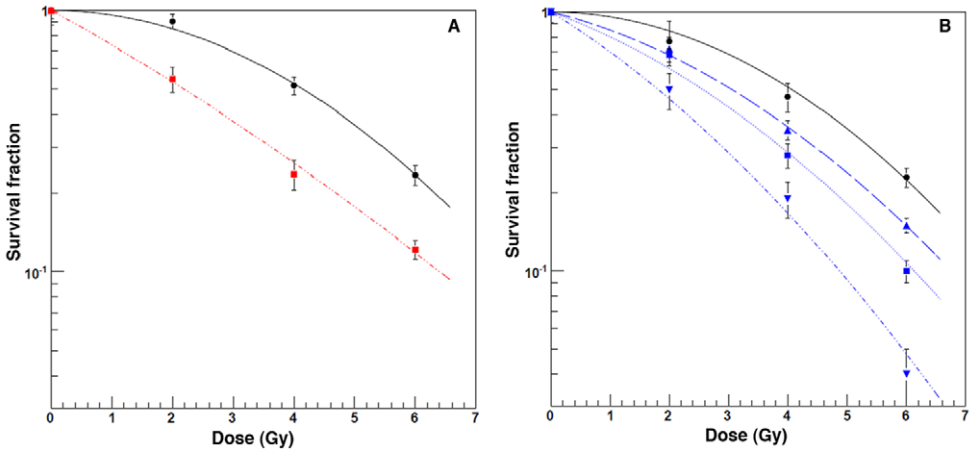

Figure 1. Radiosensitizing effects of GdNPs and GdCA. All irradiations were performed with 51 keV monochromatic x-rays. (A) F98 survival curves for untreated cells (●) and those incubated for 5 h with 2.1 mg mL^{-1} of GdNPs (■), dashed line. (B) F98 survival curves for untreated cells (●) and those irradiated in presence of 2.1 mg mL^{-1} (▲), 5.0 mg mL^{-1} (■) and 10.0 mg mL^{-1} (▼) of GdCA.

$$SF_{control} = \exp(-\alpha D - \beta D^2) \quad (3)$$

$$SF_{Gd} = \exp(-\alpha D \times DEF - \beta (D \times DEF)^2) \quad (4)$$

$$SER = SF_{control}/SF_{Gd} \quad (5)$$

$$SER = \exp(\alpha D \times (DEF - 1) + \beta D^2 \ (DEF^2 - 1)) \quad (6)$$

where:

- SF_{Gd} and $SF_{control}$, the normalized survival fractions measured experimentally with and without Gd, respectively.
- α and β were the control cells radiosensitivity parameters (in absence of radio-sensitizer) extracted from the $SF_{control}$ curve using the LQ model.
- DEF was calculated using Monte Carlo simulations, as previously described.

Results

Radiosensitization versus radiation dose, measured above the Gadolinium K-edge

In order to assess the radiosensitization potential of GdNPs, F98 glioma cells were incubated for 5 h with 2.1 mg mL^{-1} of GdNPs, then irradiated with a monochromatic photon beam at 51 keV. F98 cells also were irradiated with 0, 2.1, 5.0 or 10.0 mg mL^{-1} of GdCA in the culture medium. The contrast agent was present only during the irradiation time (~20 min). At 0 Gy, SF of F98 cells incubated with GdNPs was 0.96 ± 0.11. The normalized survival values with the contrast agent were 1.00 ± 0.15, 1.01 ± 0.15, 1.08 ± 0.17 and 1.07 ± 0.14, for the four increasing GdCA concentrations respectively, indicating that both agents were non-toxic in these experimental conditions. The survival curves versus x-ray dose are shown in figure 1.

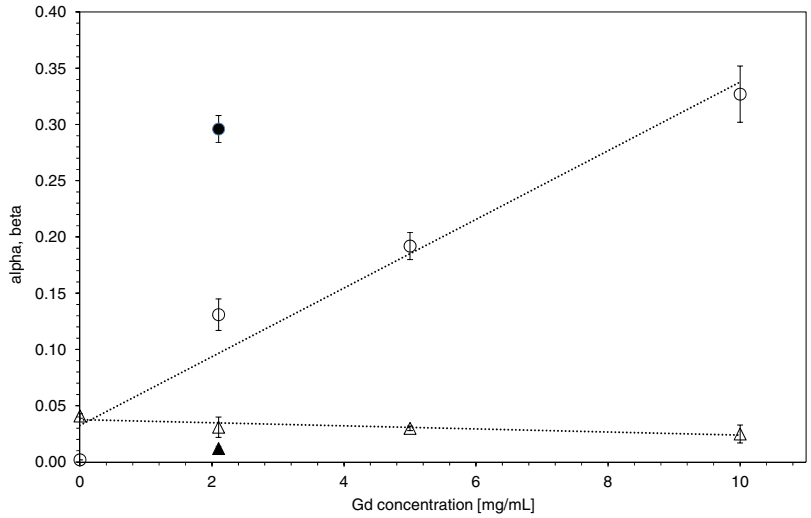

Figure 2. α (Gy^{-1}) and β (Gy^{-2}) parameters derived from the linear quadratic fits of survival curves for F98 cells treated with 2.1 mg mL^{-1} of GdNPs (●) and (▲), for α and β, respectively or 0, 2.1, 5.0 and 10.0 mg mL^{-1} of GdCA (○) and (Δ), for α and β, respectively. The irradiations were performed with 51 keV monochromatic x-rays. For GdCA, the plots of α and β versus Gd concentrations were both adjusted with a linear function (dotted lines, $R^2 > 0.95$).

The largest impact on cell survival was observed with GdCA 10 mg Gd mL^{-1}. In all cases radiosensitization was observed with Gd-treated cells. The cell radiosensitivity parameters α and β are shown in figure 2 for control and treated cells. Both GdNPs and GdCA produced a large increase of the linear parameter α, and a decrease of β. For GdCA, the increase in α depended on the Gd concentration (figures 1 and 2). The SERs in presence of Gd versus the radiation dose are shown in figure 3. The SERs reach a plateau after 5 Gy, when cells were irradiated in presence of GdNPs. In contrast, the SERs increased in the presence of GdCA, both as a function of Gd concentration and x-ray dose.

Radiosensitization versus photon energy

Figure 4 shows the theoretical SER versus the energy calculated for various x-ray doses: 1, 2, 4 and 6 Gy, with a theoretical DEF corresponding to 2.1 mg Gd mL^{-1} according to the formalism previously described (equations (1)–(5)). These results highlight the importance of the x-ray dose choice for the evaluation of the SER versus the x-ray energy. At 1 and 2 Gy, the SER variations would be too small to be measured using clonogenic assays. In the present study, the radiosensitization was evaluated experimentally at 4 Gy versus the x-ray energy.

Figure 5 summarizes the SER_{4Gy} measured for GdNPs and GdCA in comparison with the theoretical SER_{4Gy}. The experimental sensitization factors for GdCA, were in good agreement with theoretical macroscopic SER_{4Gy} at all energies (mean relative difference <10%). As expected, the greatest enhancement was obtained at 65 keV and no radiosensitization was observed when irradiation was performed at a higher energy (1.25 MeV) (figure 5).

Significantly higher SER_{4Gy} values were obtained when cells were irradiated in presence of GdNPs compared to GdCA at all energies. The highest sensitization enhancements were

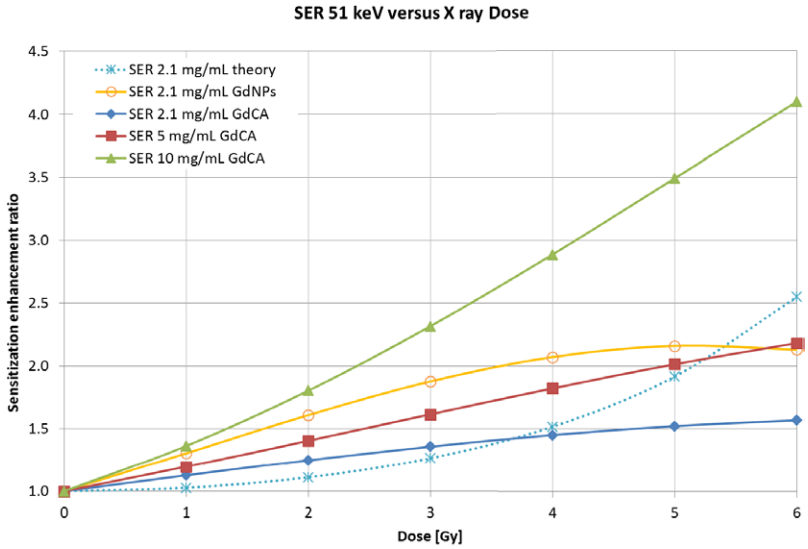

Figure 3. Sensitization-enhancement ratios versus x-ray dose. All irradiations were performed with 51 keV monochromatic x-rays.

- F98 cells incubated for 5 h with 2.1 mg mL^{-1} of GdNPs (○);
- F98 cells irradiated in presence of 2.1 mg mL^{-1} (◆), 5.0 mg mL^{-1} (■) and 10.0 mg mL^{-1} (▲) of GdCA.
- The theoretical SER for 2.1 mg mL^{-1} Gd was also plotted (*X*), dashed line.

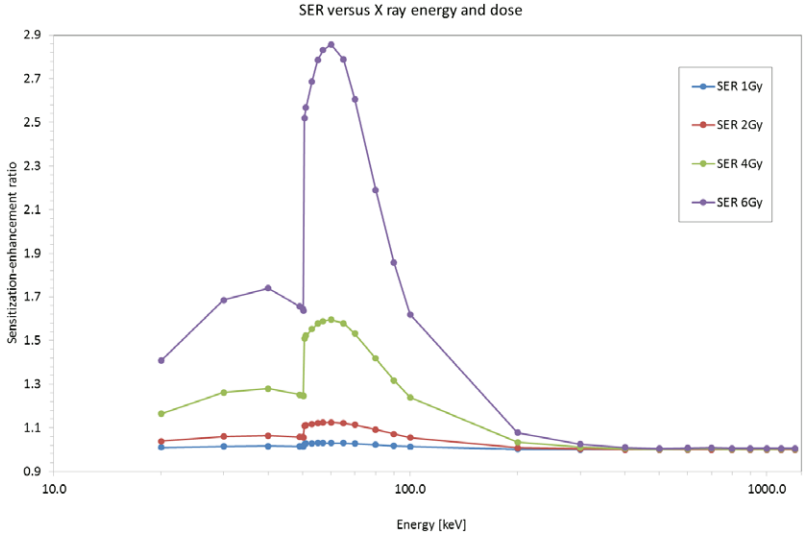

Figure 4. F98 cells' theoretical SERs calculated versus x-ray energies with 2.1 mg mL^{-1} Gd, for radiation doses of 1, 2, 4 and 6 Gy.

obtained when the cells were irradiated at 65 keV. A significant increase of the SER_{4Gy} was observed above and below the Gd K-edge (50.25 keV). GdNPs also led to a radiosensitizing effect for high-energy irradiations, which was not observed with GdCA.

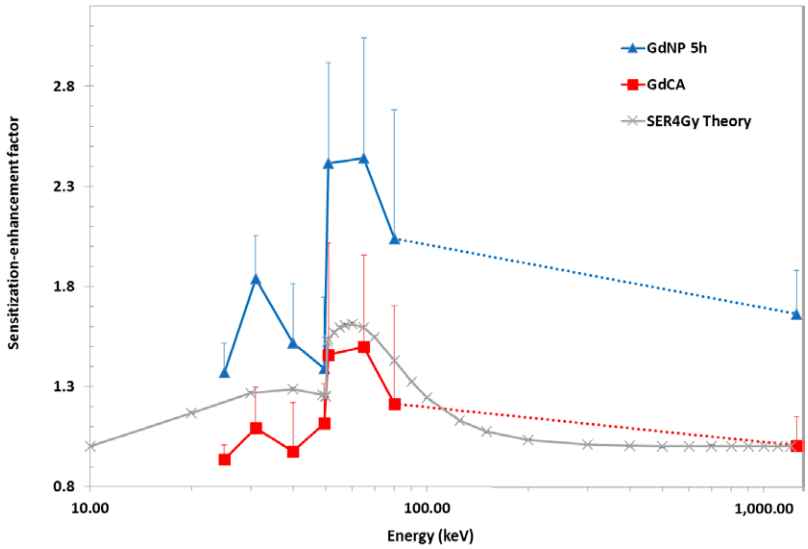

Figure 5. SER_{4Gy} of F98 cells irradiated at various x-ray energies with Gd (2.1 mg mL^{-1}). Theoretical SER_{4Gy} calculated for a homogeneous distribution of Gd, compared to SER_{4Gy} of F98 cells irradiated in the presence of either GdCA; GdNPs incubated for 5 h.

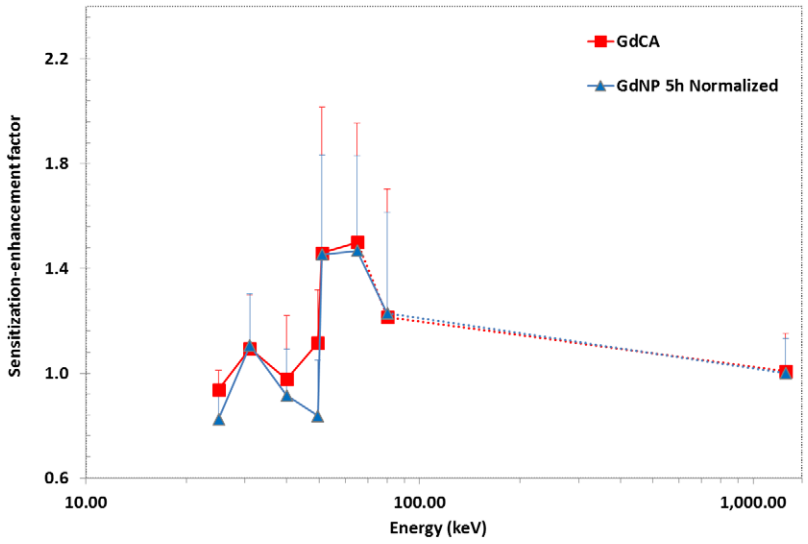

Figure 6. Comparison of the SER_{4Gy}normalized with the SER at 1.25 MeV, for GdCA and GdNPS. The relative differences (d) between the SER values are less than 5%, except at 25 and 49.5 keV where the relative differences are 11.9% and 25%, respectively (d = (SER_{GdCA} − normalized SER_{GdNP})/SER_{GdCA}).

Figure 6 shows the SER_{4Gy} in presence of GdCA, in comparison with the SER_{4Gy} obtained after incubation with GdNPs, normalized to its value measured at 1.25 MeV (SER_{4Gy} GdNPs = 1.66). Interestingly, the two plots were not significantly different. The relative differences are

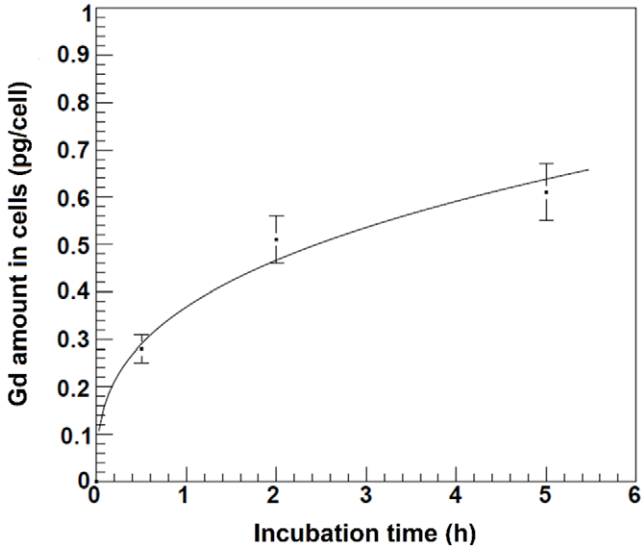

Figure 7. Uptake of GdNPs by F98 cells as a function of the incubation time (t), as determined by ICP-MS. Data were adjusted by $\alpha.t^{\beta}$, with $\alpha = 0.37 \pm 0.03$, $\beta = 0.34 \pm 0.05$ and $\chi^2 = 1.1$.

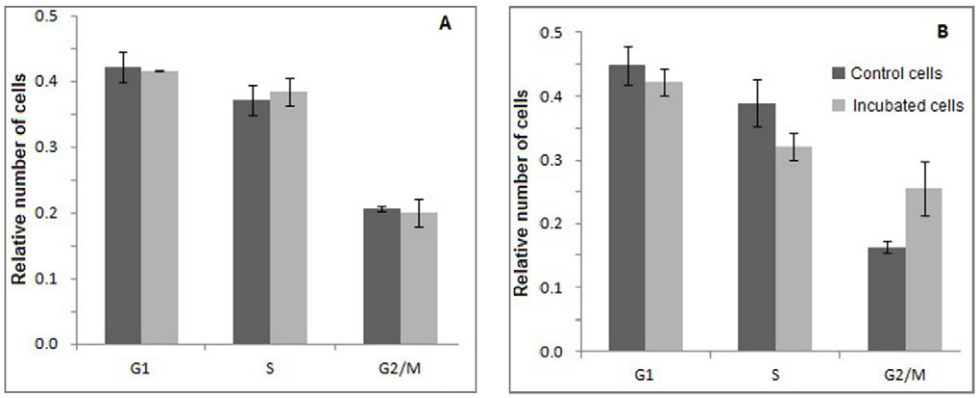

Figure 8. Distribution of F98 cells in the different phases of the cell cycle (G1, S and G2/M) for untreated controls (dark grey) and those incubated for 5 h at 37 °C with 2.1 mg mL^{-1} GdNPs (light grey). (A) Cell cycle distribution immediately after 5 h incubation. (B) Cell cycle distribution at 24 h after the end of the incubation period.

smaller than 5% for all the x-ray energies, except for 25 keV and 49.5 keV, where the relative differences were 11.9 and 25.0%, respectively (relative difference = (SER_{GdCA}-SER_{GdNPs})/SER_{GdCA}). We concluded that radiosensitization induced by GdNPs was a combination of two distinct effects: One follows the theoretical macroscopic SER variations, in a similar manner to the SER_{4Gy} of Gd contrast agent at the same concentration. The second radiosensitzation mechanism was found to be independent of the irradiation energy (factor 1.66).

Gd quantification

The kinetics for the uptake of GdNPs by F98 cells was determined by means of ICP-MS. The amount of Gd increased up to 0.60 ± 0.06 pg Gd/cell after 5 h of incubation at 37 °C with GdNPs at a concentration of 2.1 mg mL^{-1} (figure 7). A recent study reported on the Gd uptake by F98 cells incubated with Magnevist® (Peters *et al* 2015). From this study we estimate that the Gd uptake by F98 cells was 0.02 pg Gd/cells in our experimental conditions (Magnevist® in the culture medium during the cells irradiation procedure at a concentration of 2.1 mg Gd mL^{-1}, for 20 min).

Cell cycle distribution

Figure 8 depicts the proportions of F98 cells in different phases of the cell cycle for control cells and those incubated for 5 h with 2.1 mg mL^{-1} of GdNPs. Immediately after incubation, no significant differences were observed between the two conditions ($p > 0.5$), for all phases (figure 8(A)), whereas 24 h after termination of the 5 h incubation with GdNPs, a significant cellular accumulation was measured in G2/M phase ($p < 0.05$) (figure 8(B)).

Discussion

The aim of the present study was to compare two forms of Gd compounds, i.e. molecular and particular, as potential radiosensitizers for obtaining the maximal dose-enhancement in radiotherapy for the treatment of brain tumors. Differences were observed between the radiosensitizing effects produced by Gd in the form of ultrasmall NPs compared to GdCA. At the same concentration (2.1 mg Gd mL^{-1}), irradiation of F98 cells after 5 h of incubation with GdNPs led to a significantly greater enhancement of radiosensitization than that produced by GdCA only present during the irradiation time (20 min) (figures 1 and 5). The experimental SER_{4Gy} was energy dependent and reached a maximum at 65 keV (energy of theoretical maximum SER) 2.44 ± 0.33, compared to 1.50 ± 0.20, for GdNPs and GdCA, respectively.

For both agents, a significant increase in the SER_{4Gy} was observed for irradiations carried out above the Gd K-edge compared to that below the K-edge. This indicated that the photoelectric effect played a major role in the observed radiosensitivity enhancement, in both cases.

Several hypotheses have been proposed in the literature for explaining the large radiosensitizing effect observed with NPs. A physical effect linked to the structure of the nanoparticles has been suggested (Leung *et al* 2011, McMahon *et al* 2011a, 2011b, 2012, Lechtman *et al* 2013). Since the secondary electrons produced in the NPs deposit most of their energy in the immediate vicinity of the NPs (few hundreds nm) they create very hot points of doses that could impair the cell organelles. However, this physical effect was always found to be strongly related to the irradiation energy (Roeske *et al* 2007, Tsiamas *et al* 2013, Mesbahi *et al* 2013, Cai *et al* 2013, Jones *et al* 2010), and was always found to be much larger in the kV energy range in comparison to MV energies. For example, with AuNPs, Lechtman *et al* reported that in order to achieve a doubling of the prescribed dose in a tumor, the amount of AuNPs required would need to be ~300 times greater for the 6 MV source compared to the lower energy brachytherapy sources (Lechtman *et al* 2011).

Biological mechanisms that make cells more sensitive to radiation also could be involved in the radiosensitizing effects of GdNPs observed in the present study with high energy x-rays. Similarly, Jain *et al* have demonstrated radiosensitization in MDA-MB-231 cells at MV x-ray

energies using AuNPs (Jain *et al* 2011). However, they noticed that the sensitization was cell-specific; they found comparable effects at kV and MV energies, no increase in DNA double-strand break formation, and AuNPs chemopotentiation with bleomycin. From these observations, they concluded that the radiosensitization was more likely linked to biological mechanisms.

In our study, the SER_{4Gy} was found to be larger than 1 for high-energy X-irradiation when cells were incubated with GdNPs (SER_{4Gy} at 1.25 MeV = 1.66). It is noteworthy that the GdNPs SER_{4Gy} after normalization with the SER_{4Gy} value measured at high energy, was not significantly different in comparison to the SER_{4Gy} measured with GdCA, (figure 6). We concluded that the radiosensitization observed after incubation for 5 h with 2.1 mg mL^{-1} GdNPs was a combination of two distinct effects: One was strongly energy dependent and followed the theoretical macroscopic SER variations, in a similar manner to the SER_{4Gy} of Gd contrast agent at the same concentration. The second effect was not energy dependent and therefore most likely were related to a biological effect. Additional experiments have been performed to measure perturbations in cellular metabolism following exposure to GdNPs. Both cell cycle regulation and cell proliferation were affected by incubation with GdNPs. Proliferation temporarily was slowed down for up to 4 d after incubation (data not shown) and an accumulation of cells in G2/M phase was observed 24 h after the end of incubation (figure 8). In a recent study, Miladi *et al* demonstrated that GdNPs (similar to the ones used in the present study) combined with a 250 kVp energy irradiation sensitized SQ20B cells *in vitro*, as well as two other HNSCC radioresistant tumor cell lines (Miladi *et al* 2015). Although they used a shorter incubation time (1 h instead of 5 h) and smaller GdNPs concentrations (0.6 mM), they demonstrated that cell death induced in response to the combined treatment was characteristic of mitotic catastrophe followed by late apoptosis in these cell lines. Other investigators have reported similar results that were cell line and NP type dependent. Coulter *et al* (2012) reported that MDA-MB-231 cells exhibited proliferation arrest and a sub-G1 accumulation after an exposure to 12 μM of 1.9 nm AuNPs, whereas L132 cells were not affected after a similar exposure.

Good agreement was obtained between the experimental data and the theoretical macroscopic SERs versus the photon energy for the contrast agent GdCA (figure 5). The average relative difference was found to be smaller than 11%. This suggests that the physical dose enhancement induced by photoelectric effects on Gd atoms was the predominant mechanism that produced cell death. As predicted theoretically by the MC simulations at a macroscopic scale, no sensitization enhancement was observed following irradiation with 1.25 MeV photons from a cobalt 60 source. At 51 keV, the radiosensitization was directly proportional to the concentration of the high Z atoms in the medium. Regarding the survival curves, the 'α' component increased linearly ($R^2 > 0.95$) with GdCA concentration (figure 2), which indicated that the main effect was due to an increase in the number of directly lethal events due to the presence of Gd. The β value was not significantly changed, indicating an intact repair of sub lethal damages (Franken and Barendsen 2014).

In presence of GdNPs, a marked increase of the linear α component was observed (factor 150 relative to controls) and the quadratic term β became negligible (figure 2). Similar results were obtained with other cells lines and GdNPs (Sancey *et al* 2014, Miladi *et al* 2015). This might be explained by the combination of dose-enhancement due to the presence of Gd together with cell stress that occurs in presence of GdNPs.

Differences of the SER between GdNPs and GdCA also were observed versus the x-ray dose as shown in figure 3. For cells irradiated in presence of nanoparticles, saturation is observed above 4 Gy (SER ~ 2 at 51 keV). These results suggest that it would be advantageous

to choose radiation doses lower than 4 Gy when using GdNPs, since the doses would be comparable to standard treatment fractionation protocols.

In the case of GdCA, the sensitization-enhancement factors continue to increase as a function of the radiation dose and the Gd concentration (SER ~ 4 at 6 Gy in presence of 10 mg mL^{-1} of GdCA). However, the measured SER_{GdCA} versus the radiation dose did not increase exponentially as the theoretical SER (figure 3), which suggests that the dose-enhancement factors decrease when the doses increase. The maximum SER_{4Gy} was obtained with GdCA at 51 keV (SER_{4Gy} = 2.9), with the highest Gd concentration tested (10 mg mL^{-1}). As expected no dose-enhancement was observed with GdCA, at high energy.

Conclusions

In the present study we have observed that F98 glioma cells took up ultrasmall GdNPs without leading to a significant decrease in survival. Uptake of GdNPs was time dependent and reached a plateau after a 5 h of incubation with 2.1 mg Gd mL^{-1}. GdNPs increased the F98 cells' radiosensitivity, primarily for keV photon energies with a larger effect than that observed with the same concentration of GdCA. Based on our data, we have concluded that radiosensitization of GdNPs could be attributed to two mechanisms. First, the photoelectric effect enhancement in the keV energy range (similar to the effect observed with the GdCA), and second to biological interactions of GdNPs with the cells. In summary, our data provide strong support for the radiosensitizing effect of Gd over a broad energy range, even at high energies such as those used in conventional radiotherapy for GdNPs. Further *in vivo* pre-clinical studies on their therapeutic efficacy, tumor uptake and toxicity are however mandatory to define the potential clinical benefit of both ultrasmall GdNPs and GdCA as radiation sensitizers.

Acknowledgments

This work was performed within the framework of the 'Labex Primes' (ANR-11-LABX-0063) of Lyon University, within the program 'Investissements d'Avenir' (ANR-11-IDEX-0007) and ANR project 'Raphaelo' ANR-2010-BLAN-1532-02 operated by the French National Research Agency (ANR). This manuscript is dedicated to the memory of Pascal Perriat, who recently passed away.

Conflict of interest

F Lux and P Perriat have one patent to disclose: WO2011135101. This patent protects the nanoparticles described in this publication; none for the other authors.

References

Barth R F and Kaur B 2009 Rat brain tumor models in experimental neuro-oncology: the C6, 9L, T9, RG2, F98, BT4C, RT-2 and CNS-1 gliomas *J. Neurooncol.* **94** 299–312

Boudou C *et al* 2005 Monte Carlo dosimetry for synchrotron stereotactic radiotherapy of brain tumours *Phys. Med. Biol.* **50** 4841–51

Boudou C *et al* 2007 Polymer gel dosimetry for synchrotron stereotactic radiotherapy and iodine dose-enhancement measurements *Phys. Med. Biol.* **52** 4881–92

Butterworth K T, Coulter J A, Jain S, Forker J, McMahon S J, Schettino G, Prise K M, Currell F J and Hirst D G 2010 Evaluation of cytotoxicity and radiation enhancement using 1.9 nm gold particles: potential application for cancer therapy *Nanotechnology* **21** 295101

Butterworth K T *et al* 2012 Physical basis and biological mechanisms of gold nanoparticle radiosensitization *Nanoscale* **4** 4830–8

Cai Z *et al* 2013 Investigation of the effects of cell model and subcellular location of gold nanoparticles on nuclear dose enhancement factors using Monte Carlo simulation *Med. Phys.* **40** 114101

Cao Y *et al* 2006 Estimate of vascular permeability and cerebral blood volume using Gd-DTPA contrast enhancement and dynamic T2*-weighted MRI *J. Magn. Reson. Imag.* **24** 288–96

Ceberg C *et al* 2012 Photon activation therapy of RG2 glioma carrying Fischer rats using stable thallium and monochromatic synchrotron radiation *Phys. Med. Biol.* **57** 8377–91

Corde S *et al* 2005 Sensitivity variation of doped Fricke gel irradiated with monochromatic synchrotron x-rays between 33.5 and 80 keV *Radiat. Prot. Dosim.* **117** 425–31

Coulter J A *et al* 2012 Cell type-dependent uptake, localization, and cytotoxicity of 1.9 nm gold nanoparticles *Int. J. Nanomed.* **7** 2673–85

De Stasio G *et al* 2001 Gadolinium in human glioblastoma cells for gadolinium neutron capture therapy *Cancer Res.* **61** 4272–7

Di Corato R *et al* 2013 High-resolution cellular MRI: gadolinium and iron oxide nanoparticles for in-depth dual-cell imaging of engineered tissue constructs *ACS Nano* **7** 7500–12

Dingfelder M *et al* 2008 Comparisons of calculations with PARTRAC and NOREC: transport of electrons in liquid water *Radiat. Res.* **169** 584–94

Franken N A and Barendsen G W 2014 Enhancement of radiation effectiveness by hyperthermia and incorporation of halogenated pyrimidines at low radiation doses as compared with high doses: implications for mechanisms *Int. J. Radiat. Biol.* **90** 313–7

Gastaldo J *et al* 2008 Normoxic polyacrylamide gel doped with iodine: response versus x-ray energy *Eur. J. Radiol.* **68** S118–20

Hainfeld J F *et al* 2010 Gold nanoparticles enhance the radiation therapy of a murine squamous cell carcinoma *Phys. Med. Biol.* **55** 3045–59

Hainfeld J F, Smilowitz H M, O'Connor M J, Dilmanian F A and Slatkin D N 2013 Gold nanoparticle imaging and radiotherapy of brain tumors in mice *Nanomedicine* **8** 1601–9

Incerti S *et al* 2010 Comparison of GEANT4 very low energy cross section models with experimental data in water *Med. Phys.* **37** 4692–708

Jain S *et al* 2011 Cell-specific radiosensitization by gold nanoparticles at megavoltage radiation energies *Int. J. Radiat. Oncol. Biol. Phys.* **79** 531–9

Jones B L, Krishnan S and Cho S H 2010 Estimation of microscopic dose enhancement factor around gold nanoparticles by Monte Carlo calculations *Med. Phys.* **37** 3809–16

Karnas S J *et al* 1999 Optimal photon energies for IUdR K-edge radiosensitization with filtered x-ray and radioisotope sources *Phys. Med. Biol.* **44** 2537–49

Karnas S J *et al* 2001 Monte Carlo simulations and measurement of DNA damage from x-ray-triggered auger cascades in iododeoxyuridine (IUdR) *Radiat. Environ. Biophys.* **40** 199–206

Lechtman E *et al* 2013 A Monte Carlo-based model of gold nanoparticle radiosensitization accounting for increased radiobiological effectiveness *Phys. Med. Biol.* **58** 3075–87

Le Duc G *et al* 2004 *In vivo* measurement of gadolinium concentration in a rat glioma model by monochromatic quantitative computed tomography—comparison between gadopentetate dimeglumine and gadobutrol *Invest. Radiol.* **39** 385–93

Le Duc G *et al* 2011 Toward an image-guided microbeam radiation therapy using gadolinium-based nanoparticles *ACS Nano* **5** 9566–74

Leung M K *et al* 2011 Irradiation of gold nanoparticles by x-rays: Monte Carlo simulation of dose enhancements and the spatial properties of the secondary electrons production *Med. Phys.* **38** 624–31

Liamsuwan T *et al* 2012 Microdosimetry of low-energy electrons *Int. J. Radiat. Biol.* **88** 899–907

Lin Y *et al* 2014 Comparing gold nano-particle enhanced radiotherapy with protons, megavoltage photons and kilovoltage photons: a Monte Carlo simulation *Phys. Med. Biol.* **59** 7675–89

Luchette M *et al* 2014 Radiation dose enhancement of gadolinium-based AGuIX nanoparticles on HeLa cells *Nanomedicine* **10** 1751–5

Lechtman E *et al* 2011 Implications on clinical scenario of gold nanoparticle radiosensitization in regards to photon energy, nanoparticle size, concentration and location *Phys. Med. Biol.* **56** 4631–47

Mesa A V *et al* 1999 Dose distributions using kilovoltage x-rays and dose enhancement from iodine contrast agents *Phys. Med. Biol.* **44** 1955–68
Mesbahi A, Jamali F and Garehaghaji N 2013 Effect of photon beam energy, gold nanoparticle size and concentration on the dose enhancement in radiation therapy *Bioimpacts* **3** 29–35
McMahon S J *et al* 2008 Radiotherapy in the presence of contrast agents: a general figure of merit and its application to gold nanoparticles *Phys. Med. Biol.* **53** 5635–51
McMahon S J *et al* 2011a Nanodosimetric effects of gold nanoparticles in megavoltage radiation therapy *Radiother. Oncol.* **100** 412–6
McMahon S J *et al* 2011b Biological consequences of nanoscale energy deposition near irradiated heavy atom nanoparticles *Sci. Rep.* **1** 18
McMahon S J, Prise K M and Currell F J 2012 Comment on 'implications on clinical scenario of gold nanoparticle radiosensitization in regards to photon energy, nanoparticle size, concentration and location' *Phys. Med. Biol.* **57** 287–90
Miladi I *et al* 2015 Combining ultrasmall gadolinium-based nanoparticles with photon irradiation overcomes radioresistance of head and neck squamous cell carcinoma *Nanomedicine* **11** 247–57
Mowat P *et al* 2011 *In vitro* radiosensitizing effects of ultrasmall gadolinium based particles on tumour cells *J. Nanosci. Nanotechnol.* **11** 7833–9
Norman A, Iwamoto K S and Cochran S T 1991 Iodinated contrast agents for brain tumor localization and radiation dose enhancement *Invest. Radiol.* **26** S120–1 (discussion S125-8)
Peters T, Grunewald C, Blaickner M, Ziegner M, Schutz C, Iffland D, Hampel G, Nawroth T and Langguth P 2015 Cellular uptake and *in vitro* antitumor efficacy of composite liposomes for neutron capture therapy *Radiat. Oncol.* **10** 342
Pignol J P *et al* 2003 Clinical significance of atomic inner shell ionization (ISI) and Auger cascade for radiosensitization using IUdR, BUdR, platinum salts, or gadolinium porphyrin compounds *Int. J. Radiat. Oncol. Biol. Phys.* **55** 1082–91
Robar J L 2006 Generation and modelling of megavoltage photon beams for contrast-enhanced radiation therapy *Phys. Med. Biol.* **51** 5487–504
Robar J L, Riccio S A and Martin M A 2002 Tumour dose enhancement using modified megavoltage photon beams and contrast media *Phys. Med. Biol.* **47** 2433–49
Roeske J C *et al* 2007 Characterization of the theorectical radiation dose enhancement from nanoparticles *Technol. Cancer Res. Treat* **6** 395–401
Sancey L *et al* 2014 The use of theranostic gadolinium-based nanoprobes to improve radiotherapy efficacy *Br. J. Radiol.* **87** 20140134
Solberg T D, Iwamoto K S and Norman A 1992 Calculation of radiation dose enhancement factors for dose enhancement therapy of brain tumours *Phys. Med. Biol.* **37** 439–43
Stefancikova L *et al* 2014 Cell localisation of gadolinium-based nanoparticles and related radiosensitising efficacy in glioblastoma cells *Cancer Nanotechnol.* **5** 6
Stupp R *et al* 2005 Radiotherapy plus concomitant and adjuvant temozolomide for glioblastoma *New Engl. J. Med.* **352** 987–96
Stupp R *et al* 2009 Effects of radiotherapy with concomitant and adjuvant temozolomide versus radiotherapy alone on survival in glioblastoma in a randomised phase III study: 5 year analysis of the EORTC-NCIC trial *Lancet Oncol.* **10** 459–66
Terrissol M, Edel S and Pomplun E 2004 Computer evaluation of direct and indirect damage induced by free and DNA-bound iodine-125 in the chromatin fibre *Int. J. Radiat. Biol.* **80** 905–8
Tsiamas P *et al* 2013 Impact of beam quality on megavoltage radiotherapy treatment techniques utilizing gold nanoparticles for dose enhancement *Phys. Med. Biol.* **58** 451–64